Check for updates

Investigation of the effects on proton relaxation times upon encapsulation in a water-soluble synthetic receptor†

Krishna N. Chaudhary,[a] Kyra I. Brosnahan,[a] Lucas J. Gibson-Elias,[b] Jose L. Moreno Jr,[b] Briana L. Hickey,[b] Richard J. Hooley [ID][b] and Bethany G. Caulkins [ID] *[a]

Sequestration of small molecule guests in the cavity of a water-soluble deep cavitand host has a variety of effects on their NMR properties. The effects of encapsulation on the longitudinal (T_1) and transverse (T_2) relaxation times of the protons in variably sized guest molecules are analyzed here, using inversion recovery and spin-echo experiments. Sequestration of neutral organic species from the bulk solvent reduces the overall proton relaxation times, but the magnitude of this effect on different protons in the same molecule has a variety of contributors, from the motion of the guest when bound, to the position of the protons in the cavity and the magnetic anisotropy induced by the aromatic walls of the host. These subtle effects can have large consequences on the environment experienced by the bound guest, and this sheds light on the nature of small molecules in enclosed environments.

Introduction

Macrocyclic cavity-containing hosts have been exploited for a variety of applications in supramolecular chemistry,[1] including catalysis[2a] biosensing,[2b–h] molecular recognition,[1,2i,j] and the study of the behavior of small molecules in confined environments.[3] Deep cavitands such as **TCC** (Fig. 1)[4] and other related deep-cavity macrocyclic hosts[5,6] are capable of confining small, neutral organic substrates in an environment separate from the bulk medium. Some effects of this confinement include enhanced reactivity,[7] and sequestration from the external medium.[8] Sequestration can lead to effects like enhanced room temperature phosphorescence of pyrene derivatives,[8d] selective protection of isomeric esters against solvolysis,[5a] and the possibility of sequential tandem catalysis.[8e]

In addition to applications in recognition, reactivity and sensing, more focused studies have been performed on the nature of confinement and its impact on the behavior of bound guests.[5,6,9] These include molecular motion, carceroisomerism, and the thermodynamics and kinetics of coencapsulation. All these studies tend to rely on NMR spectroscopy, as it is sensitive, capable of monitoring kinetics, and the signals for

bound substrate are often separated from the peaks for the receptor, simplifying analysis.

One facet of the encapsulation event that is rarely explored is the effect of binding on the relaxation rates of individual nuclei.
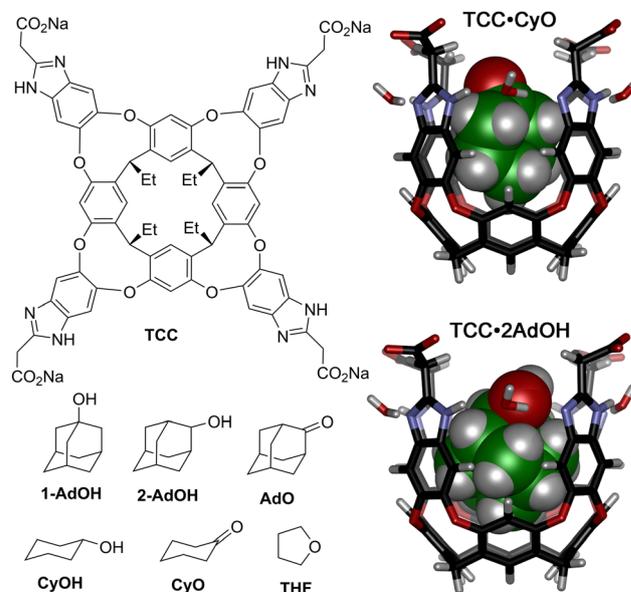

Fig. 1 (a) Cavitand and guest structure; (b) minimized structure of the **TCC·CyO**, **TCC·2AdOH** complexes (lower rim groups truncated for clarity, SPARTAN 20, AMBER forcefield).

[a] *Department of Natural Sciences, Pitzer and Scripps Colleges, Claremont, California, 91711, USA. E-mail: BCaulkins@scrippscollege.edu*

[b] *Department of Chemistry, University of California–Riverside, Riverside, CA 92521, USA*

Guest relaxation rates are often required in the process of optimizing signal for chemical exchange experiments such as GEST or NOESY/EXSY,[9a,10] but studies on the effect of binding inside a defined cavity on the individual longitudinal (T_1) and transverse (T_2) relaxation times[11] of bound protons are rarer.

Longitudinal, or spin–lattice (T_1) relaxation describes the return to thermal equilibrium population states, and occurs *via* mechanisms whereby excited spins transfer the energy obtained from the RF pulse to the surrounding medium as heat, often *via* collisions, vibrations, and rotations with surrounding solvent molecules.[11a–c] The T_1 relaxation mechanism can be expected to be influenced most strongly by encapsulation of a guest molecule inside a synthetic cavity, as the surrounding environment is highly different from bulk solvent and motion is hindered. Transverse, or spin–spin (T_2) relaxation occurs *via* a dephasing of the spins due to inhomogeneities in the local magnetic field and is often induced by spin exchange processes with surrounding molecules[11d,e] The effects of encapsulation on this mechanism are less obvious, as the bulk magnetic field (and any related inhomogeneities) can still be felt by the guest once bound, and the guest is still in close contact with other atoms, allowing for spin exchange processes to continue.

We set out to understand both the global effect of binding on T_1/T_2 times, and whether those differences were dependent on positioning inside the host cavity. For example, when substrates are bound in **TCC**, the magnetic anisotropy of the cavity increases as guest resides closer to the cavitand base. This affects the chemical shift, with the relevant $\Delta\delta$ values of bound protons in *n*-decanol ranging from −0.0 ppm at the upper rim to −5.0 ppm at the base.[9c] The effect of this variable anisotropy on the relaxation times of bound protons is not known, however. Here, we perform a study on the variations on both longitudinal and transverse relaxation times of a variety of cyclic, neutral organic guests upon encapsulation inside the **TCC** host in aqueous solution and show that both the longitudinal and transverse relaxation properties of guests can be controlled by their size- and shape-fitting inside the host.

Results and discussion

For a complete discussion of the experimental techniques and acquisition parameters used for these experiments, please see the ESI.† The first task was to determine suitable guests that would allow comparison of the T_1/T_2 times of multiple individual protons when bound. While **TCC** is quite a promiscuous host, this task introduces a set of restrictions on the substrate pool. The guests must be soluble at approximately millimolar concentration in water in the absence of cavitand, they must obviously form kinetically stable inclusion complexes with the host, and the protons must be differentiable by NMR spectroscopy in both the free and bound forms to allow for determination of T_1 and T_2 relaxation times and their direct comparison.

The molecular recognition properties of the water-soluble deep cavitand **TCC** (Fig. 1) have been well-studied,[4,9] and the scope of suitable guests is well-known. Guest encapsulation is determined by a combination of hydrophobicity and guest size: linear alkanes can coil into a helix to maximize the cavity occupancy, and hydrocarbons from *n*-pentane to *n*-tridecane can be bound, along with a series of branched variants.[9a] Cyclic hydrocarbons are preorganized into structures that favorably fill the cavity, and cycloalkanes from C_5–C_{12} bind strongly, as well as polycyclic species such as decalins, alkylcycloalkanes, pinenes and norbornanes are suitable substrates. However, while the parent hydrocarbons are good guests, they are poorly suited for our task, in that they are either sparingly soluble in free water or show minimal separation of the relevant protons in either the bound or free states. As such, we focused on alkyl ketones and alkanols: these show differentiation in chemical shift in the free state, are freely soluble in water, and generally occupy one stable configuration inside the host (as opposed to unfunctionalized hydrocarbons). Other functional groups such as halogens, thiols or carboxylic acids are possible, but can have complex structures upon binding in the host.[9c]

The guests chosen are shown in Fig. 1: they consist of cyclic hydrocarbons that are sufficiently water-soluble to obtain relaxation data in aqueous solution, bind strongly in the cavitand[9a] ($K_a > 10^4$ M^{-1}), and show easily differentiated proton signals in both the bound and free states. These differentiated protons are shown in Fig. 2. When bound in **TCC**, additional differentiation in the proton signal is observed. For example, in **2-AdOH**, there is overlap between the various methylene protons in water, but all the protons are fully differentiated when bound in **TCC** (see Fig. 3; for full spectra and peak assignments, see ESI†).

The six chosen guests vary in their NMR complexity and binding properties. **THF** is the smallest guest and shows broad peaks when bound due to rapid tumbling inside the cavity. The two cyclohexyl guests **CyO** and **CyOH** show more defined peaks, and are orientationally restricted when bound: the polar oxygens are oriented towards the bulk solvent, and a single carceroisomer is seen. The guest rotates rapidly around the vertical axis while bound, but shows no "up/down" rotation. In addition, no peaks for the axial conformer of **CyOH** can be seen, as only the equatorial conformer is present at any appreciable concentration in the cavity.[9d] The adamantane guests are interesting, as there are two orientations that they can display. The "usual" orientation of 1-substituted adamantanes in cavities such as these[9a,12] is for the polar group to be pointed vertically, as illustrated for **1-AdOH** in Fig. 2a. This positions the H_d protons vertically downward in the cavity, and they feel the greatest magnetic anisotropy and have the furthest upfield shift upon binding. However, for **AdO** and **2-AdOH**, the polar group is positioned at the 2-position, which favors a different conformation while bound (illustrated in Fig. 2) that positions the terminal methylene ($H_{d'}$, H_i in **AdO** and **2-AdOH**, respectively) at the cavitand base. Again, all the adamantyl derivatives freely rotate about the vertical axis of the cavitand while bound, but are restricted in their up/down rotation, so only one carceroisomer is seen. Finally, **2-AdOH** and **CyOH** contain prochiral centers, so they display more ^{1}H NMR signals for

10184 | *Phys. Chem. Chem. Phys.,* 2024, **26**, 10183–10190

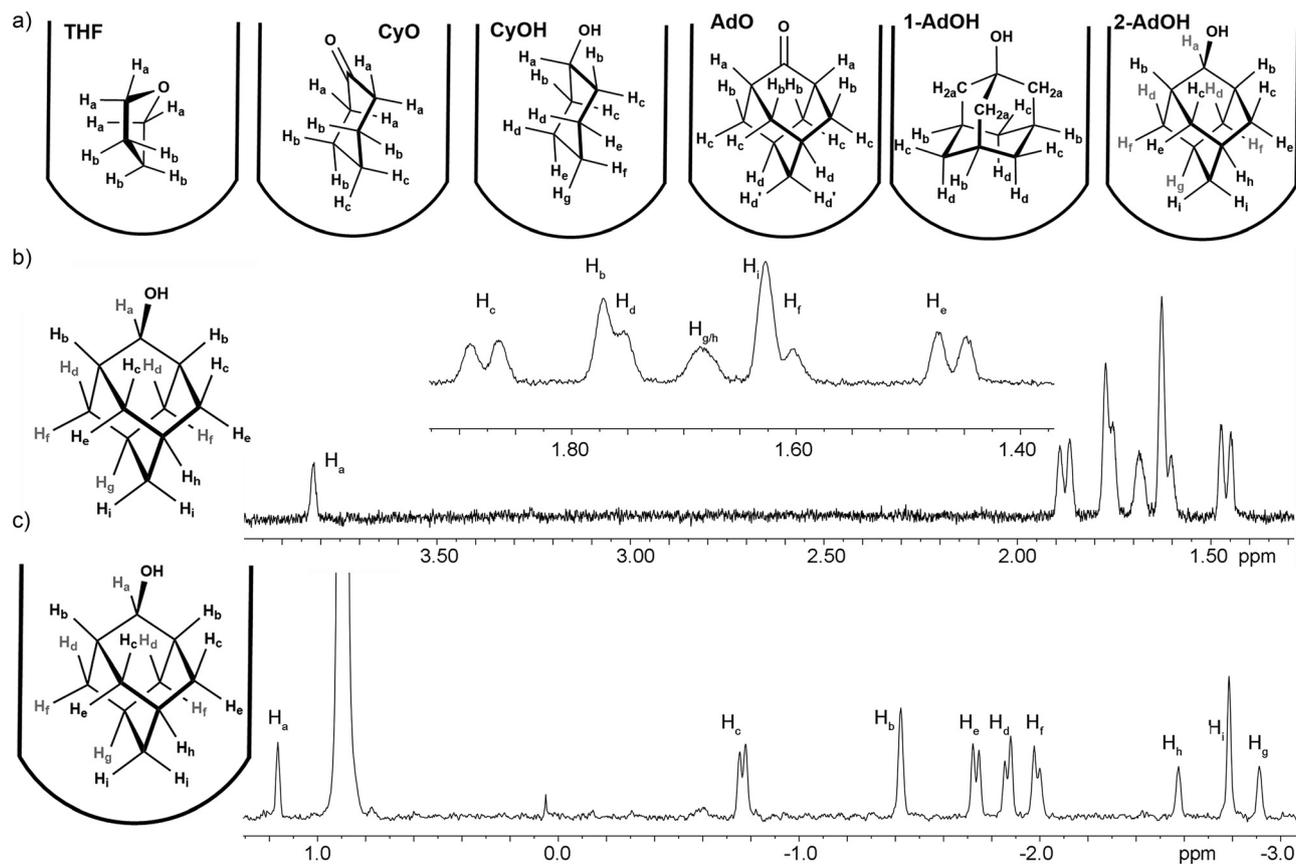This journal is © the Owner Societies 2024

Fig. 2 (a) Labeled structures of guests bound in **TCC**. ^{1}H NMR spectra and labeled peak assignments of (b) **2-AdOH**; (c) **2-AdOH·TCC** (400 MHz, D$_2$O, 298 K, [**TCC**] = 2 mM).

the diastereotopic protons on certain methylenes. These are clearly differentiated inside the cavitand, although there is some overlap in free solution. The spectra were assigned based on analysis of the ^{1}H spectra, as well as incorporating some 2D NOESY and COSY analysis to confirm the assignment. For full 1D spectra containing peak assignments, see ESI.†

The longitudinal relaxation times (T_1) for all six guests were determined using a one-dimensional inversion recovery experiment.[13] Experiments were performed on a 11.7-T Bruker Avance III spectrometer (^{1}H resonance: 500.13 MHz). Delay times in the experiment varied from 0 s to 3 s, depending on system and the amount of time it took for signals to turn negative. The T_1 value for each discrete, separable proton in D$_2$O both while free and while bound to **TCC** was determined by plotting the resulting spectral data in Mathematica and fitting it to eqn (1). The data are shown in Fig. 3 and Table 1 (for additional data, see ESI†).

$$M(t) = M_0 - 2M_0 e^{-t/T_1} \tag{1}$$

Error values were determined by plotting the residuals for each data point collected. The absolute value of the mean of the residual values was divided by the mean of the signal intensity to find a percent error for each relaxation time.

The initial, simplest observation from the T_1 data in Table 1 is that the time for longitudinal relaxation is significantly shorter when bound in the cavity than it is in free solution. While there is variation in the T_1 times between different protons at different positions in the same guest (for example, protons near heavy atoms such as O have a longer T_1 than those that are remote), a consistent variation between bound and free protons can be seen. In each case, the observed [1]H T_1 when bound is ~ 0.5–2 s shorter than it is for the same proton free in solution. Looking more closely, some other trends can be observed: firstly, the ΔT_1 is not affected in any appreciable way by the depth of the proton in the cavitand. For example, the H$_a$ protons in **1-AdOH**, which are positioned at the upper rim of the cavitand, show exactly the same ΔT_1 as the H$_d$ protons, which are oriented vertically downwards at the base of the cavity. This trend is repeated for the other guests, too.

The most notable trend is the global difference in T_1 between protons on differently sized molecules, and this can be surprisingly large. For example, ΔT_1 for **AdO** is between 2–2.4 s, whereas for **2-AdOH**, which is almost exactly the same size as **AdO** and should occupy the same orientation in the cavity, the ΔT_1 values are between 0.8–1.3 s. These data indicate that the observed T_1 values of guest bound inside the cavity are, in some cases, almost independent of the T_1 values observed in free solution. The protons in **2-AdOH** in water have a much shorter relaxation time (1.3–2.2 s) than those in **AdO** (2.7–3.7 s), but when bound in **TCC**, the T_1 values become quite similar
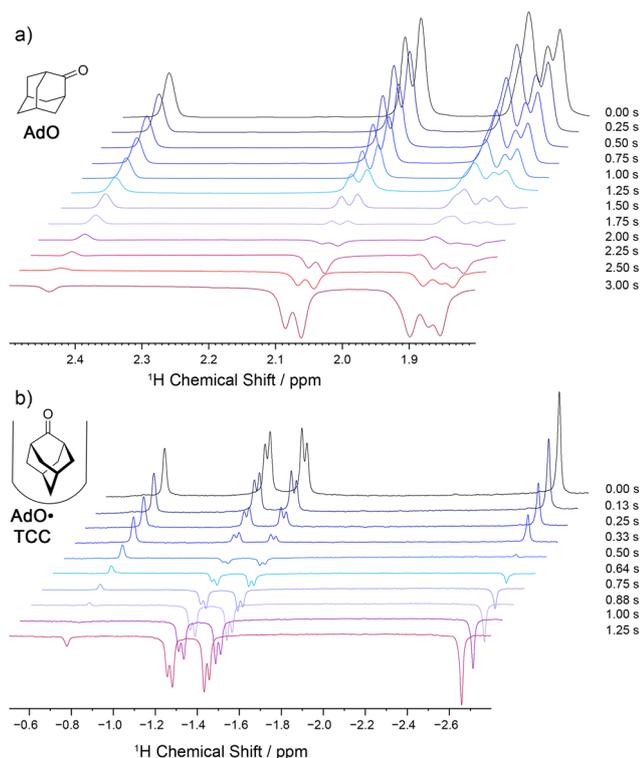
This journal is © the Owner Societies 2024

Phys. Chem. Chem. Phys., 2024, **26**, 10183–10190 | **10185**

a)

b)

Fig. 3 Stacked NMR spectra for the inversion recovery experiments determining T_1 for **AdO**, (a) free in D_2O and (b) bound in **TCC** in D_2O, [**TCC**] = 2 mM, [**AdO**] = 3 mM, D_2O, 500 MHz, 298 K.

Table 1 Longitudinal relaxation times (T_1, sec) for guests when bound in host **TCC** or free in D_2O solution[a]

Guest proton	T_1 (free), s	T_1 (bound), s	ΔT_1
CyO			
H_a	3.04 ± 0.13	2.02 ± 0.16	1.02 ± 0.21
H_b	2.69 ± 0.21	1.90 ± 0.13	0.79 ± 0.25
H_c	2.74 ± 0.24	1.99 ± 0.22	0.75 ± 0.33
AdO			
H_a	3.72 ± 0.14	1.34 ± 0.10	2.38 ± 0.17
H_b	2.74 ± 0.15	0.579 ± 0.026	2.16 ± 0.15
H_c	2.96 ± 0.10	0.554 ± 0.024	2.41 ± 0.10
H_d	2.70 ± 0.17	0.732 ± 0.021	1.97 ± 0.17
CyOH			
H_a	3.02 ± 0.03	1.86 ± 0.09	1.16 ± 0.09
H_b	2.10 ± 0.04	1.12 ± 0.08	0.98 ± 0.09
H_c	2.03 ± 0.04	1.12 ± 0.09	0.91 ± 0.10
H_d	2.07 ± 0.05	1.04 ± 0.18	1.03 ± 0.11
H_e	2.03 ± 0.05	1.06 ± 0.08	0.97 ± 0.09
H_f	2.03 ± 0.04	0.973 ± 0.06	1.06 ± 0.07
H_g	2.10 ± 0.04	0.979 ± 0.10	1.12 ± 0.11
1-AdOH			
H_a	1.66 ± 0.07	1.17 ± 0.03	0.49 ± 0.08
H_b	2.18 ± 0.07	1.63 ± 0.08	0.55 ± 0.11
H_c	1.41 ± 0.06	0.962 ± 0.049	0.45 ± 0.08
H_d	1.44 ± 0.06	0.976 ± 0.053	0.46 ± 0.08
2-AdOH			
H_a	2.23 ± 0.71	0.908 ± 0.17	1.32 ± 0.73
H_b	1.93 ± 0.45	1.04 ± 0.069	0.89 ± 0.46
H_c	1.36 ± 0.51	0.488 ± 0.045	0.87 ± 0.51
H_d	1.79 ± 0.45	0.493 ± 0.037	1.29 ± 0.45
H_e	1.38 ± 0.48	0.471 ± 0.043	0.91 ± 0.48
H_f	1.60 ± 0.54	0.506 ± 0.036	1.09 ± 0.54
H_g	1.85 ± 0.59	1.01 ± 0.16	0.84 ± 0.61
H_h	1.85 ± 0.59	1.02 ± 0.17	0.83 ± 0.61
H_i	1.77 ± 0.34	0.572 ± 0.032	1.20 ± 0.34
THF			
H_a	3.73 ± 0.27	1.52 ± 0.07	2.21 ± 0.28
H_b	3.66 ± 0.26	1.57 ± 0.05	2.09 ± 0.26

[a] Spectra were recorded using the inversion recovery pulse sequence, [**TCC**] = 2 mM, [added guest] = 3 mM, D_2O, 500 MHz, 298 K. Data were fit in Mathematica to extract the relaxation parameters. $\Delta T_1 = T_1$ (free) − T_1 (bound).

(0.5–1 s, with H_a in **AdO** being the sole outlier). This observation is not completely consistent, especially for **CyO** and **CyOH**, which have a large difference in bound T_1 ($\Delta\Delta T_1 \sim 1$ s), but it is consistent for the large adamantyl guests.

These observations suggest a theory for the changes in proton T_1 upon guest binding in the cavitand. For longitudinal relaxation, the relaxation time is determined by how easily the nuclei can transfer the excited state thermal energy to the surrounding lattice as they return to their equilibrium population states. As we are comparing the relative T_1s for protons in their bound and free states, any variations from molecular structure (the presence of heavy atoms, functional groups, C *vs.* H, *etc.*) should not apply. Differences between bound and free states can stem from (a) differential rotation of the molecule; (b) variations in the "solvation" shell (water *vs.* the aromatic walls of the cavitand); (c) effective compression of the molecule, which affects C–H vibrational modes; (d) magnetic anisotropy effects from the host; (e) protection from external dissolved oxygen in the solvent while bound.[8d] Not all of these differences are large, or even important, but all could contribute to changes in T_1 time.

The data in Table 1 indicate that the relative size and shape of the guest controls the observed T_1 values. In free D_2O solution, the CH protons in the alcohols (**CyOH**, **1-AdOH**, **2-AdOH**) show significantly shorter T_1 times than the ketones (**CyO**, **AdO**) or **THF**. This is likely due to more favorable hydrogen bonding between the OH group and water, allowing more rapid transfer of thermal energy to the surrounding solvent. To address the question of the effect of water on free guest, we determined the T_1 relaxation data for **1-AdOH** and **2-AdOH** in other organic solvents, tetrachloroethane-d_2 and DMSO-d_6 (see ESI† for data). These measurements show that T_1 values for these alcohols are slower in TCE (a non-hydrogen-bonding solvent) than in either water or DMSO, corroborating the theory.

When in the cavitand, the guest is shielded from water, and this effect is attenuated. Now, the energy transfer must occur between the guest and the cavitand walls, which is determined by how close the guest protons are to the host aromatic groups. Interestingly, this effect appears to be independent of the magnetic anisotropy field in the cavitand: T_1 times inside the **TCC** cavity are not dependent on the vertical position (*i.e.*, depth) in the cavity, as chemical shifts are, but on the relative proximity to the cavitand walls. The wider guests (**AdO**, **1-AdOH**, **2-AdOH**), generally show shorter T_1 times than the smaller cyclohexanes (**CyO**, **CyOH**), and much shorter bound T_1 times than the small **THF**. These effects are illustrated more starkly upon closer inspection of the individual protons. The comparison between the protons in **AdO** and **2-AdOH** is most
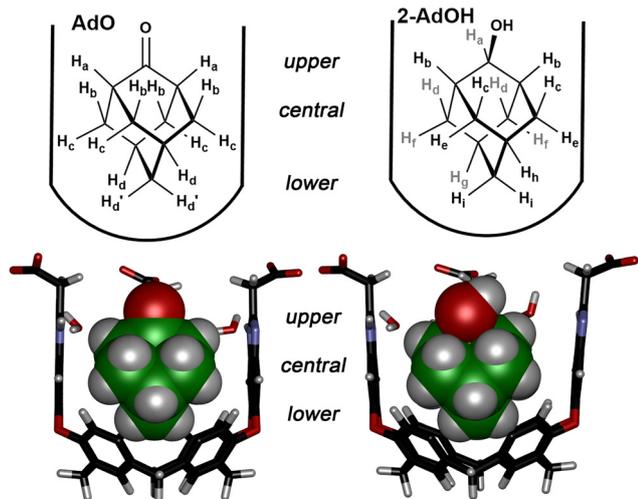
10186 | *Phys. Chem. Chem. Phys.*, 2024, **26**, 10183–10190

This journal is © the Owner Societies 2024

Fig. 4   Bound host guest structures and proton positioning for **AdO·TCC** and **2-AdOH·TCC**. Structures minimized in SPARTAN '20, AMBER force-field, front walls and lower rim feet removed for clarity.

illustrative (see Fig. 4). The different protons can be separated into 3 groups – "upper" protons that may have contact with bulk water (H_a in **AdO**, H_a/H_b in **2-AdOH**), "central" protons that interact with the cavitand walls (H_b/H_c in **AdO**, $H_c - H_f$ in **2-AdOH**), and "lower" protons that point to the cavity base (H_d in **AdO**, $H_g - H_h$ in **2-AdOH**). The observed T_1 values for these almost identical protons are also almost identical. The only variation is for the lower protons, where the signal for H_d in **AdO** encompasses two different proton types, so the T_1 is averaged. In both cases, the "central" and "lower" protons have similar T_1 times, controlled by their position in the host. The fastest T_1s occur for the "central" protons, oriented directly at the sidewalls, and the T_1 for the "lower" protons is slightly longer. The upper protons have longer T_1 values, as they are exposed to bulk solvent and show relaxations more reminiscent of bulk solution, *i.e.* the difference in T_1 for "upper" bound protons and their free counterparts is much less than the difference between those in the depths of the cavity. This could be due to collisions with solvent or a greater exposure to external O_2 in the solvent; either way, the "upper" environment is more similar to the external milieu than the "lower" interior of the cavity.

This effect is less obvious for the smaller, more rapidly tumbling guests such as **CyO** and **THF**. As **CyO** is fluxional and averages signals for the axial/equatorial protons (which are discrete in **CyOH**), a similar "direct comparison" analysis is not possible. However, the general concept of the cavitand providing its own solvation shell that controls T_1 values is still broadly valid. Interestingly, there does not appear to be a large difference between axial and equatorial protons in bound **CyOH**, although the "upper" proton H_a shows a longer T_1 than the others, corroborating the results seen for **AdO/2-AdOH**, whereby protons that are exposed to solvent show a longer T_1 than those buried in the cavity.

The data in Table 1 indicate that the T_1 relaxation of guests is controlled by thermal energy transfer to the host, which

introduces the question of whether there are any effects of guest size on the T_1 relaxation times of the host protons. The T_1 times for the four different sets of protons on the cavitand (the benzimidazole CH, the two different resorcinarene aromatic CH, and the lower rim methine) were calculated in the presence of three differently sized guests (**THF**, **CyOH** and **AdO**, see ESI† for data). Interestingly, there is almost no change at all in the T_1 times with various guests: the T_1 time for the methine varies from 1.21 s (**AdO**) to 1.26 s (**CyOH**). The only change that could be seen was for the side-wall benzimidazole CH atoms, which go from 1.51 s (**THF**) to 1.64 s (**AdO**). This might be an indication that the walls are distorted somewhat by the larger guest (an observation seen previously[9a]), but the change is so small that this is purely speculative. The exposure of the cavitand to bulk solvent with or without guests bound may explain the lack of a change in T_1 values between systems.

In addition to determining T_1 times for bound guests, we also analyzed T_2. Specifically, T_2* ($T_2* = T_2 + T_2 (\Delta B_0)$) was measured, so magnetic field inhomogeneity is included in the measurement, although the samples were scrupulously shimmed to limit the effects of this. The transverse relaxation times (T_2) for the six guests were determined using the Hahn spin echo experiment.[14] Spectra were recorded on a 11.7-T Bruker Avance III spectrometer (^{1}H resonance: 500.13 MHz). T_2 relaxation times were significantly faster than the T_1 times, so delay times in the experiment varied from 0 ms to 50 ms, depending on system and the amount of time it took for signals to diminish. The T_2 value for each discrete, separable proton in D_2O both while free and while bound to **TCC** was determined by plotting the resulting spectral data in Mathematica and fitting it to eqn (2).

$$M(t) = M_0 e^{-t/T_2} \qquad (2)$$

Error values were determined by plotting the residuals for each data point collected. The mean of the residual values was divided by the mean of the signal intensity to find a percent error for each relaxation time. The data are shown in Fig. 5 and Table 2. The T_2 times were significantly shorter than T_1 times (as expected[15]), so the data in Table 2 is shown in msec.

As the transverse relaxation mechanism is different from that for longitudinal relaxation, it was not immediately clear what the effect of guest encapsulation would be. The data in Table 2 do show some clear trends, however. In most cases, the T_2 relaxation times of bound guest protons are shorter than their counterparts in free D_2O solution. This is not completely consistent, however, and changes with the nature of guest. For example, the smallest, fastest tumbling guests **THF** and **CyO** show markedly shorter T_2 times when bound than free in solution: for **THF**, the relaxation is almost an order of magnitude faster (∼100 ms free, 10 ms bound). In contrast, the larger guests show much smaller changes: the ΔT_2 values for the protons in **AdO** and **2-AdOH** change by only ∼20%, and some protons actually show an increase in T_2 relaxation time.

Upon closer inspection, more information can be gleaned. The "upper" protons in the bound guests show a longer T_2 time than the protons that are more buried inside the cavity, similar
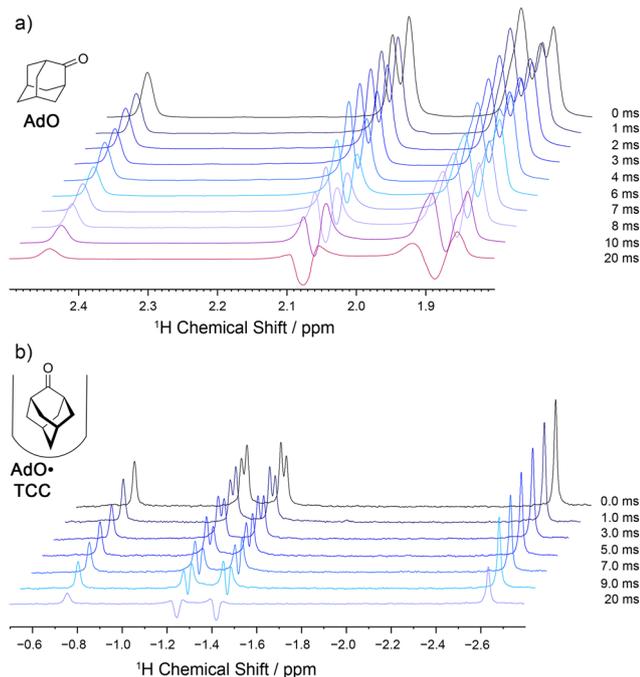
This journal is © the Owner Societies 2024

Phys. Chem. Chem. Phys., 2024, **26**, 10183–10190 | **10187**

Fig. 5 Stacked NMR spectra for the CPMG-1D spin echo experiments determining T_2 for **AdO**, (a) free in D_2O and (b) bound in **TCC** in D_2O, [**TCC**] = 2 mM, [**AdO**] = 3 mM, D_2O, 500 MHz, 298 K.

Table 2 Transverse relaxation times (T_2, sec) for guests when bound in host **TCC** or free in D_2O solution[a]

Guest proton	T_2 (free), ms	T_2 (bound), ms	ΔT_2
CyO			
H_a	36.9 ± 2.0	12.6 ± 0.7	24.3 ± 2.1
H_b	14.0 ± 0.5	8.73 ± 0.55	5.3 ± 0.7
H_c	29.4 ± 3.3	9.89 ± 0.40	19.5 ± 3.3
AdO			
H_a	21.3 ± 0.1	21.6 ± 0.7	−0.3 ± 0.7
H_b	9.90 ± 0.60	8.53 ± 0.14	1.37 ± 0.62
H_c	14.8 ± 0.5	9.84 ± 0.21	4.96 ± 0.54
H_d	24.9 ± 3.0	30.5 ± 0.8	−5.6 ± 3.1
CyOH			
H_a	13.8 ± 0.8	8.74 ± 0.64	5.1 ± 1.0
H_b	13.5 ± 0.5	9.89 ± 0.50	3.6 ± 0.7
H_c	11.9 ± 0.6	8.23 ± 0.39	3.7 ± 0.7
H_d	10.4 ± 0.6	7.02 ± 0.36	3.4 ± 0.7
H_e	13.5 ± 0.6	8.25 ± 0.41	5.3 ± 0.7
H_f	7.93 ± 0.51	6.26 ± 0.38	1.67 ± 0.64
H_g	9.89 ± 0.51	9.06 ± 0.56	0.83 ± 0.76
1-AdOH			
H_a	36.6 ± 1.3	28.6 ± 0.9	8.0 ± 1.6
H_b	18.0 ± 0.7	16.5 ± 1.0	1.5 ± 1.2
H_c	11.5 ± 0.7	9.01 ± 0.46	2.5 ± 0.8
H_d	12.1 ± 0.8	9.64 ± 0.40	2.5 ± 0.9
2-AdOH			
H_a	28.2 ± 1.7	18.4 ± 2.6	9.8 ± 3.1
H_b	15.0 ± 1.4	16.4 ± 1.3	−1.4 ± 1.9
H_c	11.9 ± 0.2	7.15 ± 0.92	4.8 ± 0.9
H_d	13.1 ± 0.3	7.13 ± 1.05	6.0 ± 1.0
H_e	14.1 ± 0.7	14.5 ± 2.3	−0.4 ± 2.4
H_f	13.4 ± 1.2	10.3 ± 0.7	3.1 ± 1.4
H_g	19.1 ± 0.9	14.4 ± 1.6	4.7 ± 1.8
H_h	19.1 ± 0.9	22.3 ± 5.2	−3.2 ± 5.3
H_i	17.2 ± 1.1	24.6 ± 1.3	−7.5 ± 1.7
THF			
H_a	91.5 ± 10.6	8.45 ± 0.75	83.1 ± 10.6
H_b	116 ± 16	10.5 ± 0.7	106 ± 16

[a] Spectra were recorded using the CPMG-1D pulse sequence, [**TCC**] = 2 mM, [added guest] = 3 mM, D_2O, 500 MHz, 298 K. Data were fit in Mathematica to extract the relaxation parameters. $\Delta T_1 = T_1$ (free) − T_1 (bound).

to the trend seen for T_1 times. This trend is not as clear as for T_1, as the data is skewed somewhat by the greater effect of heavy atoms on nearby protons and the larger differences in free T_2 time. However, the general observation is relatively consistent, that "upper" protons show T_2 times closer to that in free solution. In contrast, the "central" protons for each guest show T_2 times that are all clustered around 10 ms (with a range of 9–10 ms). This applies to almost all the guests, no matter their width, exchange, or tumbling rate – the "central" protons in **AdO**, **CyO**, **CyOH**, **THF** and **1-AdOH** are all in this range, with only **2-AdOH** as the outlier (but in this case, the difference is small, with T_2 ranging from 10–14 ms). The other outliers are the "lower" protons, especially in **AdO** and **2-AdOH**, which show much longer T_2 relaxation.

From this, a plausible theory can be postulated: evidently the induced magnetic field displayed by the aromatic rings in the cavitand (and the concomitant magnetic anisotropy in the cavity) is a mini-magnetic field that "smooths" the anisotropies felt by the bound guest protons and evens out T_2 relaxation times. This effect is seen most strongly for protons that reside in the "central" position. The smallest effects are seen for "upper" protons, similar to the observations for T_1, as these protons experience more of the bulk medium than their "central" counterparts. The guest molecule experiences a more uniform magnetic environment while bound in **TCC**, so the T_2 relaxation times for each proton all fall into a narrower range. There are outliers, and the prevalence of external factors (such as defects in the NMR tube, any small particulate impurities in the sample, or dissolved O_2) that can affect the T_2 time make the data less amenable to interpretation than the T_1 data.

However, the general effect of encapsulation of different types of guests is again quite clear and quite substantial.

The same kind of "smoothing" can also be caused by changes in molecular motion, and this is seen mostly clearly for the fast-tumbling guests **THF** and **CyO**. In free solution, these guests show long T_2 relaxation times, consistent with greater dynamics than the other, larger guests.[11e,15,16] However, when bound in the cavitand, the motion of all the guests is controlled by the constricted cavity, and therefore the overall T_2 times are far more uniform, and there are fewer differences between the observed times for different guests.

An important question when analyzing the T_1 and T_2 relaxation data is whether the results are solely for "bound" guests, or whether in/out exchange occurs on a timescale that would lead to differential contributions from the bound state. The exchange rates for bound guests in **TCC** are relatively constant, and dependent on guest size and overall hydrophobic surface area. Larger guests exchange more slowly than smaller ones, and the exchange rates in **TCC** for most of the guests shown in Fig. 1 (and other similarly sized species) have been previously determined.[9a] They range from k = 9.8 s^{-1} (**CyO**) to k = 1.8 s^{-1}

10188 | *Phys. Chem. Chem. Phys.*, 2024, **26**, 10183–10190

This journal is © the Owner Societies 2024

(**1-AdOH**), corresponding to exchange $\Delta G^{\ddagger}$ = 16–17 kcal mol^{-1} at ambient temperature (see ESI† and ref. 9*a*). As the exchange rate is faster than the observed T_1 values, it could contribute to some "averaging" of T_1 between bound and free states. The T_2 relaxation is far faster than any exchange, though, so it can be expected to have minimal impact on the measurements.

However, as can be seen from Tables 1 and 2, the largest changes between bound and free states are seen in the measurements of T_1, where we would expect averaging to occur (if it did). It is notable that the **TCC**·guest samples were made with minimal excess guest in the system, so in each case >95% of the guest in the sample resides in the cavity. In addition, there is no obvious correlation between fast and slow exchanging guests and the observed ΔT_1 values – fast-exchanging **CyO** has a greater ΔT_1 than slow-exchanging **1-AdOH**, for example. Therefore, while we cannot rule out some variations in observed T_1 based on chemical exchange, they do not appear to be large in this case.

Conclusions

In conclusion, we have shown that the relaxation rates of different protons in small cyclic and polycyclic guests can be significantly affected by encapsulation in a water-soluble synthetic receptor. The factors that control the changes in T_1 and T_2 times are quite varied, but most of the effects fall in the same general category of "sequestration of the substrate from the bulk". The subtle positioning of different protons inside the host cavity is a strong determinant of observed T_1 relaxation time: if the protons are even slightly exposed to solvent, the observed T_1 is much closer to that experienced in bulk water, but if the proton is fully sequestered in the cavity, its relative proximity to the host walls becomes dominant. In contrast, T_2 relaxation times are mainly controlled by the induced field generated by the cavity, although proximity to bulk solvent is also important in this case. These results are unique to this particular host: other types of receptors will affect the relaxation of bound guests in different ways, depending on access to bulk solvent when bound and the type of molecular structure that surrounds the substrate. Considering the importance of complex NMR experiments that can analyze motion and behavior of substrates in confined environments, be they enzyme-substrate or synthetic host:guest complexes, and the need for optimized T_1/T_2 data for greatest efficacy, we believe these results are an important datapoint for further development of complex NMR-based experiments that can interrogate molecular recognition processes in detail.

Conflicts of interest

There are no conflicts to declare.

Acknowledgements

References

1 (*a*) F. Hof, S. L. Craig, C. Nuckolls and J. Rebek, Jr., *Angew. Chem., Int. Ed.*, 2002, **41**, 1488–1508; (*b*) R. Pinalli, A. Pedrini and E. Dalcanale, *Chem. Soc. Rev.*, 2018, **47**, 7006–7026; (*c*) Z. Laughrey and B. C. Gibb, *Chem. Soc. Rev.*, 2011, **40**, 363–386.

2 (*a*) R. J. Hooley and J. Rebek, Jr., *Chem. Biol.*, 2009, **16**, 255–264; (*b*) S. van Dun, C. Ottmann, L.-G. Milroy and L. Brunsveld, *J. Am. Chem. Soc.*, 2017, **139**, 13960–13968; (*c*) W. Zhong and R. J. Hooley, *Acc. Chem. Res.*, 2022, **55**, 1035–1046; (*d*) E. E. Harrison, B. A. Carpenter, L. E. St. Louis, A. G. Mullins and M. L. Waters, *J. Am. Chem. Soc.*, 2021, **143**, 14845–14854; (*e*) E. E. Harrison and M. L. Waters, *Chem. Sci.*, 2023, **14**, 928–936; (*f*) S. A. Minaker, K. D. Daze, M. C. Ma and F. Hof, *J. Am. Chem. Soc.*, 2012, **134**, 11674–11680; (*g*) M. A. Beatty, J. Borges-González, N. J. Sinclair, A. T. Pye and F. Hof, *J. Am. Chem. Soc.*, 2018, **140**, 3500–3504; (*h*) A. J. Selinger and F. Hof, *Angew. Chem., Int. Ed.*, 2023, **62**, e202312407; (*i*) S. Liu, H. Gan, A. T. Hermann, S. W. Rick and B. C. Gibb, *Nat. Chem.*, 2010, **2**, 847–852; (*j*) M. R. Sullivan and B. C. Gibb, *Org. Biomol. Chem.*, 2015, **13**, 1869–1877.

3 (*a*) J. Rebek Jr, *Acc. Chem. Res.*, 2009, **42**, 1660–1668; (*b*) J. H. Jordan and B. C. Gibb, *Chem. Soc. Rev.*, 2015, **44**, 547–585.

4 (*a*) S. M. Biros, E. C. Ullrich, F. Hof, L. Trembleau and J. Rebek Jr., *J. Am. Chem. Soc.*, 2004, **126**, 2870–2876; (*b*) F. Hof, L. Trembleau, E. C. Ullrich and J. Rebek Jr., *Angew. Chem., Int. Ed.*, 2003, **42**, 3150–3153.

5 (*a*) S. Liu, H. Gan, A. T. Hermann, S. W. Rick and B. C. Gibb, *Nat. Chem.*, 2010, **2**, 847–852; (*b*) M. R. Sullivan and B. C. Gibb, *Org. Biomol. Chem.*, 2015, **13**, 1869–1877; (*c*) S. Liu, D. H. Russell, N. F. Zinnel and B. C. Gibb, *J. Am. Chem. Soc.*, 2013, **135**, 4314–4324; (*d*) C. L. Gibb and B. C. Gibb, *Chem. Commun.*, 2007, 1635–1637.

6 (*a*) A. Asadi, D. Ajami and J. Rebek Jr., *J. Am. Chem. Soc.*, 2011, **133**, 10682–10684; (*b*) D. Ajami and J. Rebek Jr., *Nat. Chem.*, 2009, **1**, 87–90; (*c*) K. D. Zhang, D. Ajami, J. V. Gavette and J. Rebek Jr., *J. Am. Chem. Soc.*, 2014, **136**, 5264–5266; (*d*) S. Mosca, Y. Yu, J. V. Gavette, K. D. Zhang and J. Rebek Jr., *J. Am. Chem. Soc.*, 2015, **137**, 14582–14585; (*e*) W. Jiang and J. Rebek Jr., *J. Am. Chem. Soc.*, 2012, **134**, 17498–17501; (*f*) A. Scarso, L. Trembleau and J. Rebek, Jr., *J. Am. Chem. Soc.*, 2004, **126**, 13512–13518.

7 (*a*) R. J. Hooley, T. Iwasawa and J. Rebek Jr., *J. Am. Chem. Soc.*, 2007, **129**, 15330–15339; (*b*) J.-L. Hou, D. Ajami and J. Rebek Jr., *J. Am. Chem. Soc.*, 2008, **130**, 7810–7811; (*c*) M. Ziegler, J. L. Brumaghim and K. N. Raymond, *Angew. Chem., Int. Ed.*, 2000, **39**, 4119–4121.

8 (*a*) S. Horiuchi, T. Murase and M. Fujita, *Angew. Chem., Int. Ed.*, 2012, **51**, 12029–12031; (*b*) V. M. Dong, D. Fiedler,

This journal is © the Owner Societies 2024

Phys. Chem. Chem. Phys., 2024, **26**, 10183–10190 | **10189**

B. Carl, R. G. Bergman and K. N. Raymond, *J. Am. Chem. Soc.*, 2006, **128**, 14464–14465; (*c*) L. S. Kaanumalle, C. L. D. Gibb, B. C. Gibb and V. Ramamurthy, *J. Am. Chem. Soc.*, 2004, **126**, 14366–14367; (*d*) C. J. Easley, M. Mettry, E. M. Moses, R. J. Hooley and C. J. Bardeen, *J. Phys. Chem. A*, 2018, **122**, 6578–6584; (*e*) Y. Ueda, H. Ito, D. Fujita and M. Fujita, *J. Am. Chem. Soc.*, 2017, **139**, 6090–6093.

9 (*a*) R. J. Hooley, H. J. Van Anda and J. Rebek, Jr., *J. Am. Chem. Soc.*, 2007, **129**, 13464–13473; (*b*) R. J. Hooley, S. M. Biros and J. Rebek, Jr., *Chem. Commun.*, 2006, 509–511; (*c*) R. J. Hooley, J. V. Gavette, D. Ajami and J. Rebek, Jr., *Chem. Sci.*, 2014, **5**, 4382–4387; (*d*) L. Perez, M. Mettry, B. G. Caulkins, L. J. Mueller and R. J. Hooley, *Chem. Sci.*, 2018, **9**, 1836–1845.

10 (*a*) L. Avram, M. A. Iron and A. Bar-Shir, *Chem. Sci.*, 2016, **7**, 6905–6909; (*b*) L. Avram, A. D. Wishard, B. C. Gibb and A. Bar-Shir, *Angew. Chem., Int. Ed.*, 2017, **56**, 15314–15318.

11 (*a*) D. L. Ashley, E. R. Barnhart, D. G. Patterson, Jr. and R. H. Hill, Jr., *Anal. Chem.*, 1988, **60**, 15–19; (*b*) E. Breitmaier, K.-H. Spohn and S. Berger, *Angew. Chem., Int. Ed. Engl.*, 1975, **14**, 144–159; (*c*) S. K. Vaish, A. Singh, A. K. Singh and N. K. Mehrotra, *Ind. J. Pure. Appl. Phys.*, 2005, **43**, 295–300; (*d*) R. M. Levy, M. Karplus and P. G. Wolynes, *J. Am. Chem. Soc.*, 1981, **103**, 5998–6011; (*e*) U. Haeberlen, U. W. Spiess and D. Schweitzer, *J. Mag. Res.*, 1972, **6**, 39–54.

12 R. J. Hooley, S. R. Shenoy and J. Rebek Jr., *Org. Lett.*, 2008, **10**, 5397–5400.

13 E. D. Becker, J. A. Ferretti, R. K. Gupta and G. H. Weiss, *J. Magn. Reson.*, 1980, **37**, 381–394.

14 E. L. Hahn, *Phys. Rev.*, 1950, **80**, 580–594.

15 T. D. W. Claridge, *High-Resolution NMR Techniques in Organic Chemistry*, Elsevier, 2nd edn, 2008.

16 B. G. Caulkins, S. A. Cervantes, J. M. Isas and A. B. Siemer, *J. Phys. Chem. B*, 2018, **122**, 9507–9515.

10190 | *Phys. Chem. Chem. Phys.*, 2024, **26**, 10183–10190

This journal is © the Owner Societies 2024